

Detailed investigation of Long-Period activity at Campi Flegrei by Convolutional Independent Component Analysis

P. Capuano^{a,c}, E. De Lauro^{b,c}, S. De Martino^b, M. Falanga^{b,*}

^a*Dept. of Physics "E.R. Caianiello", Salerno University, Giovanni Paolo II, 132, 84084, Fisciano (SA), Italy*

^b*Dept. of Computer Eng. and Electrical Eng. and Applied Mathematics, Salerno University, Giovanni Paolo II, 132, 84084, Fisciano (SA), Italy*

^c*AMRA Scarl, Via Nuova Agnano 11, Napoli, Italy*

Abstract

This work is devoted to the analysis of seismic signals continuously recorded at Campi Flegrei Caldera (Italy) during the entire year 2006. The radiation pattern associated with the Long-Period energy release is investigated. We adopt an innovative Independent Component Analysis algorithm for convolutional seismic series adapted and improved to give automatic procedures for detecting seismic events often buried in the high-level ambient noise. The extracted waveforms characterized by an improved signal-to-noise ratio allows the recognition of Long-Period precursors, evidencing that the seismic activity accompanying the mini-uplift crisis (in 2006), which climaxed in the three days from 26 - 28 October, had already started at the beginning of the month of October and lasted until mid of November. Hence, a more complete seismic catalog is then provided which can be used to properly quantify the seismic energy release. To better ground our results, we first check the

*Corresponding author, E-mail: mfalanga@unisa.it

robustness of the method by comparing it with other blind source separation methods based on higher order statistics; secondly, we reconstruct the radiation patterns of the extracted Long-Period events in order to link the individuated signals directly to the sources. We take advantage from Convolutional Independent Component Analysis that provides basic signals along the three directions of motion so that a direct polarization analysis can be performed with no other filtering procedures. We show that the extracted signals are mainly composed of P waves with radial polarization pointing to the seismic source of the main LP swarm, i.e. a small area in the Solfatara, also in the case of the small-events, that both precede and follow the main activity. From a dynamical point of view, they can be described by two degrees of freedom, indicating a low-level of complexity associated with the vibrations from a superficial hydrothermal system. Our results allow us to move towards a full description of the complexity of the source, which can be used, by means of the small-intensity precursors, for hazard-model development and forecast-model testing, showing an illustrative example of the applicability of the CICA method to regions with low seismicity in high ambient noise.

1. Introduction

1 The classification of seismic signals occurring on active volcanoes is rele-
2 vant in discriminating those that can be considered strictly related to the dy-
3 namics of a volcano from various other external influences. Indeed, the detec-
4 tion of specific signals such as Long-Period (LP) events or explosion-quakes
5 or the prompt recognition of the resurgence of volcanic tremor is very relevant

6 (see, e.g., Konstantinou and Schlindwein 2002; Kawakatsu and Yamamoto,
7 2007) because these signals are associated with the source mechanism and
8 often appear in the pre-syn eruptive process. In addition, an increase in the
9 number and/or in the amplitude of such signals may reveal a variation of
10 the dynamical state of the volcano, implying a different contribution of the
11 seismic energy involved in the process. The latter could give new insights on
12 the general modeling and shed light onto the nature of seismic events such
13 as LPs often associated with the renewing activity (see, e.g., Chouet and
14 Julian, 1985; Julian, 1994; Neuberg et al., 2000; Bean et al., 2014). Anyway,
15 the accuracy of automatic procedures for detecting seismic events and lo-
16 cating their sources is influenced by many factors including errors in seismic
17 phases picking, events that are often buried in the high-level ambient noise,
18 network geometry, and even variability in the waveforms. So, a significant
19 objective is the improvement of detection procedures by developing accurate
20 algorithms for quasi-real time seismic data processing, easily manageable in
21 observatory practice: the most important advantages are their consistency
22 and their capability of processing large datasets such as those produced for
23 monitoring densely-populated volcanic areas. Many efforts have been made
24 to solve that problem both from a theoretical point of view and from devel-
25 oping numerical algorithms suitable for specific cases with the main aim to
26 clearly identify the P-phase (refer to, e.g., Kao et al., 2007; Rouland et al.,
27 2009; Küperkoch et al., 2010; Moni et al., 2013). As an alternative approach,
28 we seek to recognize and extract all the waveforms. A detailed review of the
29 methodologies adopted to perform decomposition and detection of relevant
30 seismic signals can be found in Carniel (2014) and references therein. This

31 work is devoted to the analysis of seismic signals continuously recorded at
32 Campi Flegrei Caldera (Italy) during the entire year 2006 which includes the
33 main LP swarm that occurred during 26-28 October, and investigating the
34 radiation patterns associated with the LP energy release. Specifically, the
35 analyzed time series are the recordings of ground velocity along the three
36 directions of motion (North-South, East-West and Vertical) for each station.
37 We adopt an innovative technique, i.e. the Convolutional Independent Com-
38 ponent Analysis (CICA) algorithm, adapted and improved to give automatic
39 procedures for detecting seismic events often buried in the high-level ambient
40 noise, as Ciaramella et al. (2011) showed investigating the limited period for
41 the most energetic activity of the swarm. The main interests are: 1) to es-
42 tablish whether the occurrence of LPs is only limited to the swarm climaxed
43 on the three days 26-28 October 2006, or a longer period is experienced; 2)
44 to investigate the radiation patterns of all events, particularly interesting in
45 the case of small-energy events. The latter exploits the capability of CICA
46 to provide basic signals eventually correlated to the main seismic phases,
47 so an immediate polarization is obtained, giving information on the source
48 mechanism. This should solve the hard problem to identify the best filter
49 bands corresponding to the fundamental and other interesting phases; 3) to
50 characterize all small events in terms of dynamical system in order to link
51 them to the main hydrothermal resonating structure.

52 To test the performance of the method to separate low-energy events
53 from noise in the pre/post climax activity, we compare CICA with a number
54 of efficient algorithms for ICA both based on second order and higher or-
55 der statistics. The extracted waveforms with improved signal-to-noise ratios

56 (SNR) via CICA coupled with automatic phase picking will allow the com-
57 pilation of a more complete seismic catalog, which could be used to better
58 quantify the seismic energy release taking into account the overall LP activ-
59 ity and characterize the source from a dynamical point of view (i.e. giving
60 the degrees of freedom of the system).

61 **2. Geological setting of Campi Flegrei and dataset**

62 The Campi Flegrei volcanic complex is a nested caldera, which originated
63 from two large collapses which occurred during the eruption of the Campa-
64 nian Ignimbrite (39 ka) and the Neapolitan Yellow Tuff (15 ka) eruptions,
65 and it is located to the West of the town of Naples (Southern Italy). The
66 caldera, characterized by a very complex structural setting (Capuano et al.,
67 2013), is affected by the phenomenon of Bradyseisms, continuous slow subsi-
68 dence, interspersed with fast ground uplifts accompanied by seismicity. The
69 most relevant recent ground deformation episodes occurred in 1969-1972 and
70 1982-1984 and generated a net uplift of 3.5 m around the town of Pozzuoli
71 (Orsi et al., 1999). Since that time, minor uplift episodes (i.e., 2000, 2005-
72 2006, 2010, 2012-2013) occurred (Saccorotti et al., 2007). The presence of
73 geothermal reservoirs plays an important role in determining the dynamics
74 of the caldera and many tomographic studies (see, e.g., De Siena et al., 2010;
75 Petrosino et al., 2012) provide evidence of fluids, whose intrusion and migra-
76 tion to the shallower hydrothermal system causes ground deformations (De
77 Natale et al., 2006). The deformation episode of 2005-2006 was characterized
78 by a large release of seismic energy and by the occurrence, in October 2006, of
79 the most remarkable LP swarm ever recorded in the area. The documented

80 LP activity lasted for about 1 week and climaxed on days 26, 27 and 28,
81 when hundreds of events were counted (Saccorotti et al., 2007; Ciaramella
82 et al., 2011). The LP signals appear like spindle-shaped monochromatic os-
83 cillations and their spectra exhibit a main peak at a frequency around 0.8
84 Hz attributed to a source effect (Cusano et al., 2008). These LP events have
85 been studied in detail and have been attributed to a fluid-rock interaction in
86 the hydrothermal system (Cusano et al., 2008; Falanga and Petrosino, 2012;
87 De Lauro et al., 2012).

88 Data used for the present analysis were collected by four broadband three-
89 component seismic stations (ASB2, AMS2, TAGG, BGNG) belonging to the
90 Campi Flegrei seismic monitoring network (see location on the map in Fig. 1),
91 managed by the "Istituto Nazionale di Geofisica e Vulcanologia-Osservatorio
92 Vesuviano (INGV-OV)" (see for details Saccorotti et al., 2007) during the
93 2006 ground uplift. Specifically, the analyzed time series are the recordings of
94 ground velocity along the three directions of motion (North-South, East-West
95 and Vertical) for each station. We study the seismic signals continuously
96 recorded during the entire year 2006 with the main purpose to detect LP
97 events (eventually buried in the noise), taking into account the remarkable
98 LP swarm, which climaxed on 26-28 October. An example of continuous
99 seismic signal recorded at four selected stations is reported in Fig. 1.

100 **3. Detection method: Convolutional Independent Component Anal-** 101 **ysis**

102 Independent Component Analysis (ICA) was proposed some years ago
103 to achieve blind source separation when the source signals are mutually sta-

104 tistically independent and mixed instantaneously with an unknown matrix
105 (Hyvärinen et al., 2001). The intuitive notion of maximum nongaussianity
106 is used in ICA estimation adopting techniques which involve higher-order
107 statistics. We remind the reader that classical measures of nongaussianity
108 are the kurtosis, the negentropy, and the mutual information. ICA in its clas-
109 sical formulation can be now considered a well established method of time
110 deconvolution for signals recorded in a variety of natural systems (Capuano
111 et al., 2011; De Lauro et al., 2005, 2009). However, many natural phenomena
112 are better modeled assuming convolutive mixtures rather than instantaneous
113 ones. For example, in seismological framework, seismic signals are thought to
114 be the convolution of a source function with path, site and the instrument re-
115 sponse. So we apply an Independent Component Analysis based approach for
116 the Blind Source Separation (BSS) of convolutive mixtures in the frequency
117 domain. Briefly, in the frequency domain, the convolution leads to products
118 so that the convolutive mixture problem is transformed into subproblems of
119 instantaneous BSS/ICA models at each frequency. The transformation in
120 the frequency domain is usually the Short Time Fourier Transform (STFT).
121 Here, the observed mixtures can be broken up into frames (which usually
122 overlap each other, to reduce artifacts at the boundaries) and each frame is
123 Fourier transformed. The complex result is added to a matrix of frequency
124 bins and then each point ($X_i(\omega, t)$) can be observed both in time and fre-
125 quency. For each frequency bin, we have, therefore, n observations, which
126 can be applied to the ICA models in the complex domain. To achieve separa-
127 tion we implement a fixed-point algorithm (FastICA) that has a convergence,
128 which is quadratic, much faster than other approaches based on the linear

129 convergence obtained by gradient methods. Finally, the permutation inde-
 130 terminacy is solved by using the Hungarian approach that has a complexity
 131 of $O(n^3)$ (Ciaramella et al., 2011).

132 3.1. Blind Source Separation and ICA

133 In various real world applications, we observe that the source signals have
 134 different time delays due to the propagation in the medium. In addition,
 135 time-delayed versions of the same source exist, due to propagation paths
 136 typically caused by reverberations from some obstacles.

In the context of convolution, the data model is given by

$$x_i(t) = \sum_{j=1}^n \sum_k a_{ikj} s_j(t-k) \quad \text{for } i = 1, \dots, n \quad (1)$$

where $x_i(t)$ represent the convolutive mixtures, $s_j(t)$ are the source signals, whereas each a_{ikj} represents a Finite Impulsive Response (FIR) filter model. To invert the convolutive mixtures $x_i(t)$, a set of similar FIR filters is typically used:

$$y_i(t) = \sum_{j=1}^n \sum_k w_{ikj} x_j(t-k) \quad \text{for } i = 1, \dots, n \quad (2)$$

The output signals $y_1(t), \dots, y_n(t)$ of the separating system are the estimates of the source signals $s_1(t), \dots, s_n(t)$ at discrete times t . The w_{ikj} 's are the coefficients of the FIR filters of the separating system. In this work, we solve the problem cast in Eq. 1 relative to convolutive mixtures of seismic sources, by using the ICA-based approach described in (Ciaramella et al., 2011 and references therein). The main idea of that approach is moving to the frequency domain in order to transform the convolution into multiplications and to apply ICA methods, in the complex domain, for instantaneous

mixtures. In the frequency domain, the data model of Eq. 1 becomes

$$X_i(\omega) = \sum_{j=1}^m A_{ij}(\omega)S_j(\omega), \text{ for } i = 1, \dots, n \quad (3)$$

137 where $X_i(\omega)$, $S_j(\omega)$ and $A_{ij}(\omega)$ are the Fourier transforms of $x_i(t)$, $s_j(t)$ and
138 $a_{ij}(t)$, respectively. Comparing Eq. 1 with Eq. 3, we note that the convolutive
139 mixture problem is transformed into subproblems of instantaneous BSS/ICA
140 models at each frequency.

141 The transformation in the frequency domain is usually the Short Time Fourier
142 Transform (STFT). Here, the observed mixtures can be broken up into frames
143 (which usually overlap each other, to reduce artifacts at the boundaries) and
144 each frame is Fourier transformed. The complex result is added to a matrix
145 of frequency bins and then each point ($X_i(\omega, t)$) can be observed both in
146 time and frequency. For each frequency bin, we have, therefore, n obser-
147 vations, to which apply the ICA models in the complex domain. For more
148 detailed description on convolutive blind source separation method refers to
149 Pedersen et al. (2008). A classical example for ICA model is the cocktail
150 party problem, in which the task is to recover speech in a room of simul-
151 taneous and independent speakers recorded by a set of microphones. The
152 idea of CICA is to transform the mixed signals (speech signals) to the time-
153 frequency domain, obtaining relative spectrograms. After that, we perform
154 a blind source separation having as input these spectrograms by standard
155 ICA, obtaining the main frequencies. Finally, the separated signals in the
156 time domain are reconstructed by inverse-FFT from the spectrograms of the
157 separated components.

158 4. Analysis of seismic activity through CICA

159 The CICA method is applied in order to determine the presence of early
160 onsets of LP activity and their effective duration, checking throughout the
161 year if clusters of LP events occur. We run the method on the hourly seismic
162 traces acquired simultaneously at the four selected stations (ASB2, AMS2,
163 BGNG, TAGG) and, independently, for the three directions of motion. An
164 example of separation is shown in Fig. 2 where transients are separated from
165 noise of both meteo-marine (spectral peaks less than 1 Hz) and anthropogenic
166 sources (spectral peaks above 1.5 Hz): extracted LPs show emergent onsets,
167 absence of shear wave arrivals, appear to be spindle-shaped monochromatic
168 oscillations and have a typical spectral content in the range 0.2-2 Hz with
169 main peak at a frequency around 0.8 Hz as reported in the literature (see, e.g.,
170 Kawakatsu and Yamamoto, 2007 and references therein). By investigating
171 the entire year 2006, CICA identifies a large number of alarms also from the
172 week of the climax. In this way we extract about 1900 alarms. In order
173 to avoid false alarms, the extracted waveforms are correlated with an LP
174 master event (occurred on 26 October at 12:18:15 UT) chosen among those
175 reported in the catalog of Saccorotti et al. (2007) (see inset of Fig. 3). We
176 only consider those events having a correlation coefficient higher than 0.7
177 with the LP master. In such a way, alarms with correlations less than 0.7,
178 which are 10% of the total alarms, are neglected. We do not exclude that
179 the events with lower correlation can be LPs but with different waveforms
180 from the master.

181 An example of extraction is reported in the lower panel of Fig. 3. Specif-
182 ically, the interested period of LP occurrence spans from the beginning of

183 October until mid November, improving the statistics of the seismic cata-
184 log compiled both by Saccorotti et al. (2007) and Ciaramella et al. (2011).
185 Indeed, the first LP catalog produced by Saccorotti et al. (2007) counted
186 about 300 events applying a trigger coincidence criterion to data recorded at
187 two seismic stations with the best signal-to-noise ratio (SNR); whereas Cia-
188 ramella et al. (2011) counted about 800 events including very small energy
189 LP events during the three days of intense activity.

190 Looking at the new catalog, one realizes that a non-negligible amount of
191 energy has been released by very small events, in agreement with Falanga
192 and Petrosino (2012), who revealed a persistent sustained activity consisting
193 of very low-energy volcanic signals. These lower energy signals have been
194 unburied from background noise by CICA thus improving the statistics of
195 picked events. The new catalog containing about 1700 events is reported in
196 Fig. 3.

197 **5. Comparison with other blind signal processing methods**

198 The extraction of signals with improved SNR is crucial for obtaining
199 precise polarization analyses and locations. In addition, the highlighting of
200 low-energy events allows a prompt detection of volcanic signals such as LPs
201 that often represent indicators of renewing activity. CICA seems to be very
202 efficient in detecting relevant signals in volcano-seismology, and this section
203 is just devoted to show the performance of the adopted method with respect
204 to a number of other efficient algorithms used for the blind source separation.
205 The choice to adopt ICA methods is based on the capability of ICA to extract
206 relevant signals from noise with a very low signal-to-noise ratio. Indeed, De

207 Lauro et al. (2005) demonstrated that deterministic harmonic signals can
208 be recognized by ICA in a noise with an amplitude 1000 times higher. We
209 select two types of suitable BSS/ICA methods: ICA algorithms exploiting
210 mutual independence based on higher order statistics (HOS) and algorithms
211 based on second order statistics (SOS), that is, exploiting spatio-temporal
212 decorrelation. Among the SOS, we select AMUSE (Algorithm for Multiple
213 Unknown Source Extraction based on eigenvalue decomposition) and SOBI
214 (Second Order Blind Identification), which are based on the eigenvalue de-
215 composition of a single/multiple time-delayed covariance matrixes. Among
216 HOS, we test the following algorithms:

- 217 • *Efficient variant of FastICA* is the version asymptotically more effi-
218 cient than the original FastICA. Indeed, it extracts features which are
219 robust to non-stationary noise contaminating the mixtures (i.e., seismic
220 signature from background noise).
- 221 • *Natural Gradient Flexible ICA* is an adaptive nonlinear ICA learning
222 algorithm. It implements a parameterized generalized Gaussian density
223 model on a natural Reimannian gradient structure to ascertain the
224 distribution of the source, and is able to process real-time mixed data
225 containing sub Gaussian and super Gaussian sources. The nonlinear
226 function of flexible ICA is controlled by a Gaussian index which is an
227 estimate of the kurtosis of the decomposition filer output.
- 228 • *Extended Robust ICA based on cumulants* is asymptotically equivariant
229 in the presence of Gaussian noise. This algorithm separates the signals
230 from an m mixture of n sources (with non zero kurtosis) in the presence

231 of Gaussian noise. This algorithm is a quasi-Newton iteration that will
232 converge to a saddle point with locally isotropic convergence, regardless
233 of the distributions of the sources.

- 234 • *Simultaneous Blind signal Extraction using cumulants* performs the si-
235 multaneous blind signal extraction of an arbitrary group of sources
236 from a rather large number of observations. It optimizes the Maximum
237 Likelihood criterium and solves the problem of separation whenever the
238 explicit knowledge of the source densities is lacking.

239 All these techniques are implemented in an existing Matlab toolbox - ICALAB
240 developed by Cichocki et al. (2003). The robustness of the results and the
241 consistency of the different algorithms for the same model (and in the same
242 mixing conditions, i.e. same seismic traces) is confirmed by a Monte Carlo
243 analysis being executed on a large number of trials (equal to 100 runs for
244 each technique on the same dataset). We have exploited the performance of
245 those methods in periods both pre and post climax, when both the intensity
246 and the occurrence of LPs are decreasing. The background noise may mask
247 the presence of LPs and standard seismic techniques, based on the clear
248 waveform identification, are failing. As an example, we report the results
249 relative to the day 24 October in Figs. 4-5 just approaching the climax. No
250 separation is clearly achieved, not by second order methods nor by higher
251 order statistics. Looking at the spectral content of the extracted components
252 (sources), LPs are not clearly separated from noise still displaying a broad-
253 band spectrum. We remind the reader that LPs show rather monochromatic
254 oscillations, with spectra typically peaked at about 0.7 Hz (Saccorotti et al.,
255 2007; Cusano et al., 2008). On the contrary, CICA application works very

256 well in separating LPs from noise as shown in Fig. 2, where the spectral
257 peak below 1 Hz is generally associated with the meteo-marine component
258 whereas the anthropogenic noise extends above 1.5 Hz.

259 **6. Recognition of temporal pattern**

260 The extraction of signals with improved SNR is crucial for obtaining
261 precise polarization analysis and locations.

262 In addition, the highlighting of low-energy events allows a prompt de-
263 tection of volcanic signals such as LPs that often represent indicators of
264 renewing activity (Aki et al., 1977; Chouet and Julian, 1985; Kumagai and
265 Chouet 1999; Neuberg et al., 2000; Kumagai et al., 2002; Nakano et al., 2003;
266 Matsubara and Yomogida, 2004; Bean et al., 2014).

267 Indeed, the volcanic nature of the extracted signals can be checked by
268 both looking at the seismological properties such as the polarization state or
269 locations and at the characteristics of the dynamical systems associated with
270 the source. In this sense, the capability of CICA to provide basic signals
271 eventually correlated to the main seismic phases allows the performing of an
272 immediate polarization analysis, avoiding "ad hoc" filtering procedures. In
273 line with these thoughts, we perform a polarization analysis on all 1700 LPs
274 of the CICA catalog. Based on the results of Falanga and Petrosino (2012),
275 who demonstrated that the LPs are composed of P waves with very shallow
276 incidence angles, we study the particle motion on the horizontal plane (NS-
277 EW). As an example, Fig. 6 shows the particle motions of a representative
278 subset of LPs at three stations with the best SNR (ASB2, AMS2, TAGG)
279 selected during the period October-November. As can be seen, polarization

280 is generally linear indicating the presence of body wave, specifically the P
281 wave, though noise can affect some results (see, e.g., TAGG which is the
282 farthest station from the source). The polarization of the first arrivals at
283 three stations can be used to locate the source: indeed, the polarization
284 vectors point towards a specific area, the Solfatara volcano, in agreement
285 with the localization of the source of LPs at about 500 m beneath (see,
286 Saccorotti et al., 2007). The method allows a much better estimate of the
287 seismic activity defining the duration of the phenomenon. In particular, a
288 clear polarization also for the low-energy events occurring at the beginning of
289 October indicates that the seismic activity had started well before the main
290 crisis.

291 A further check on the LP nature of the events extracted by CICA can
292 be performed by looking at the dynamical properties. Indeed, LPs can be
293 described by a low-dimensional dynamical system (two degrees of freedom),
294 while ambient noise unrelated to volcanic activity is higher dimensional pro-
295 cess (Falanga and Petrosino, 2012). In order to extract information about
296 the effective number of degrees of freedom of the dynamics, we explore the
297 phase space in which presumably their asymptotic dynamics evolve. We
298 adopt the averaged mutual information (AMI) (Fraser and Swinney, 1986)
299 and the false nearest neighbours (FNN) techniques (Kennel et al., 1992) to
300 estimate the time delay and the dimension of the phase space (embedding di-
301 mension), respectively. The time delay corresponds to the time lag at which
302 the AMI attains the first minimum; the embedding dimension corresponds to
303 the value at which the percentage of FNN approaches zero. The results are
304 reported in Fig. 7 in which the percentage of FNN (estimated on the basis of

305 the time lag derived from AMI) is plotted against the embedding dimension:
306 a two-dimension phase space is clearly solved indicating that these signals are
307 very low-dimensional as one expects for LPs in agreement with the results
308 of Falanga and Petrosino (2012). Similar techniques have revealed dimen-
309 sions as higher as 7-8 relative to e.g. the volcanic tremor Events Recorded
310 at Vatnajökull Volcano, central Iceland (Konstantinou, 2002).

311 **7. Discussion and conclusions**

312 The presence of LP seismicity in a volcano affords the opportunity for
313 studying the plumbing system because the seismicity may be caused by pres-
314 sure fluctuations in magmatic and hydrothermal systems beneath a volcano.
315 Swarms of LP seismic events are recognized as a precursory phenomenon for
316 the eruptive activity and are indicators of renewing activity (Chouet, 1996).
317 LP events have been interpreted as indicators of fluid presence and migration
318 in terms of linear resonances of fluid-filled cracks or cavities (Aki et al., 1977;
319 Chouet and Julian, 1985; Kumagai and Chouet 1999; Neuberg et al., 2000;
320 Kumagai et al., 2002; Nakano et al., 2003; Matsubara and Yomogida, 2004)
321 or nonlinear flow-induced oscillations in channels transporting volcanic flu-
322 ids (Julian, 1994; Rust et al., 2004). LP events with different energies may
323 depend on the magnitude of the pressure drop in the system (Chouet, 1996)
324 and changes in the flow regime may be related to different excitation levels
325 of the system (Arciniega-Ceballos et al., 2003). Furthermore, recent stud-
326 ies conducted on three active volcanoes (Etna-Italy, Turrialba volcano-Costa
327 Rica, Ubinas volcano-Peru) indicate that LP events may also be triggered
328 without any fluid and connected with the deformations of poorly consoli-

329 dated topmost layers of volcanic edifice (Bean et al., 2014; Eyre et a., 2015;
330 Thun et al., 2015). In the light of that scientific debate, the prompt identifi-
331 cation of very low-energy LPs become more relevant because it adds further
332 information on their nature, allowing a deeper understanding of the physical
333 processes involved. This topic could be a key contribution in the eruption
334 forecasting. At Campi Flegrei, LP events were never observed before the
335 2000 year ground deformation (Saccorotti et al., 2001; Bianco et al., 2004),
336 although they are commonly detected in active volcanic/hydrothermal areas;
337 the events detected in October 2006 currently constitute the most remarkable
338 LP swarm ever recorded in the area. For sake of completeness, "a posterio-
339 ri", D'Auria et al. (2011) recognized the occurrence of an ambiguous LP
340 episode, which occurred in the year 1982. In this area, these deformations can
341 be ascribed to nonlinear resonances of conduits or branches in the uppermost
342 hydrothermal system (De Lauro et al., 2012). Indeed, the 2005-2006 defor-
343 mation episode has been attributed to two hot fluid batches injected from a
344 deeper reservoir below the Pozzuoli bay, reaching the surface at Pozzuoli and
345 Solfatara area (D'Auria et al., 2012). On the other hand, all the activity of
346 the shallow geothermal reservoir generates a sustained hydrothermal tremor
347 as reported in De Lauro et al. (2013). The role of fluids is further supported
348 by geochemical studies, which have revealed an increase of the flow rate at
349 the fumaroles of Solfatara in connection with the main LP swarm (see, e.g.,
350 Chiodini et al., 2010).

351 In this work, we show an improved and more complete analysis of LP
352 activity at Solfatara volcano, Campi Flegrei (Southern Italy), investigating
353 continuous seismic signals spanning the entire year 2006 including the climax

354 26-28 October, by means of innovative techniques. We adopt an Independent
355 Component Analysis algorithm for convolutive (CICA) seismic series adapted
356 and improved to give automatic procedures for detecting seismic events often
357 buried in the high-level ambient noise. Summarizing, our study shows:

- 358 1. the existence of low-energy LP precursors provide evidence that the
359 seismic activity accompanying the mini-uplift crisis (in 2006), which
360 climaxed in one week at the end of October, started as early as at the
361 beginning of the month of October and lasted until mid November.
362 Hence, a more complete seismic catalog is then provided which can
363 be used to properly quantify the seismic energy release and eventually
364 to connect the occurrence of the LP events to the deformative history
365 of the caldera. Indeed, during the mini-uplift period, most energy is
366 released in August-September together with an increased fumarolic gas
367 emission (see, e.g., Chiodini et al., 2010), whereas the uplift ends in
368 December;
- 369 2. that CICA extracts basic signals from recordings along the three direc-
370 tions of motion. This is particularly important because it allows objec-
371 tive identification of the polarization parameters without pre-processing
372 the data by filtering procedures that often distort the signals, prevent-
373 ing blind information about the source;
- 374 3. that the extracted signals are superficial events mainly composed of
375 P waves with radial polarization pointing to the seismic source of the
376 main LP swarm, i.e. a small area in the Solfatara. This also applies to
377 the small-events that both precede and follow the main activity;
- 378 4. that very-low energy LPs can be described by two degrees of freedom

379 dynamical system similar to those of the main swarm, indicating the
380 same low complexity associated with the vibrations from superficial
381 hydrothermal system.

382 The identification and characterization of LP precursors permits better
383 highlighting the features of the hydrothermal system. Indeed, the presence
384 of a long preparatory period that leads to a mini-uplift at Campi Flegrei,
385 whose climax lasted for only a few days, and a detailed study of the low-level
386 seismicity associated with this initial period, can shed light on the renewing
387 of the activity. Moreover, such low-energy LP events appear to be generated
388 by the same superficial dendritic network of branches of a hydrothermal sys-
389 tem identified by Falanga and Petrosino (2012) and De Lauro et al. (2012),
390 implying that this system was already acting before the climax. From this
391 point of view, a detailed investigation of the stress-tensor could give infor-
392 mation on the formation and propagation of fracturing cracks. It would be
393 appropriate to re-analyze the previous time series to check retrospectively the
394 features highlighted in the year 2006, in particular in correspondence with
395 other periods of uplift and changes in other parameters, such as chemical
396 trends. This analysis would allow the verification of whether the absence of
397 LPs before year 2000 is real or due to a lack detection because of less sensi-
398 tive techniques unable to extract small events buried in the noise. Finally,
399 from a methodological point of view our technique is well-suited to detect tran-
400 sient events and should be extended to short duration (seconds to minutes)
401 episodes of tremor, which also represent indicators of renewing activity. Our
402 method holds promise for improvement of early warning procedures.

8. Acknowledgments

We are sincerely grateful the Mobile Seismic Network of the INGV-OV for having provided the data. This paper has been supported by MEDSUV EU project. This project is funded under the call FP7 ENV.2012.6.4-2, grant agreement *n*^o308665.

References

- [1] Aki, K., Fehler, M., Das, S., 1977. Source mechanism of volcanic tremor: fluid-driven crack models and their application to the 1963 Kilauea eruption. *J. Volcanol. Geoth. Res.* 2, 259-287.
- [2] Arciniega-Ceballos, A., Chouet, B., Dawson, P., 2003. Long-period events and tremor at Popocatepetl volcano (1994-2000) and their broadband characteristics. *Bull. Volc.*, 65, 124–135.
- [3] Bean, C., De Barros, L., Lokmer, I., Metaxian, J. P., O'Brien, G., and Murphy, S., 2014. Long-period seismicity in the shallow volcanic edifice formed from slow-rupture earthquakes. *Nat. Geo.* 7, 7175. doi: 10.1038/ngeo2027.
- [4] Bianco, F., Del Pezzo, E., Saccorotti, G., Ventura, G., 2004. The role of hydrothermal fluids in triggering the July-August 2000 seismic swarm at Campi Flegrei, (Italy): evidences from seismological and mesostructural data. *J. Volcanol. Geoth. Res.*, 133, 229–246.
- [5] Capuano, P., Russo, G., Civetta, L., Orsi, G., D'Antonio, M., Moretti, R., 2013. The active portion of the Campi Flegrei caldera structure

- imaged by 3-D inversion of gravity data. *Geochem. Geophys. Geosys.*, 14, 46814697, doi: 10.1002/ggge.20276
- [6] Capuano, P., De Lauro, E., De Martino, S., Falanga, M. 2011. Water-level oscillations in the Adriatic Sea as coherent self-oscillations inferred by Independent Component Analysis. *Progr. Ocean.*, 91, 447-460, doi: 10.1016/j.pocean.2011.06.001.
- [7] Carniel, R. 2014. Characterization of volcanic regimes and identification of significant transitions using geophysical data: a review. *Bull Volcanol.*, 76,848, doi:10.1007/s00445-014-0848-0
- [8] Chiodini, G., Caliro, S., Cardellini, C., Granieri, D., Avino, R., Baldini, A., Donnini, M., Minopoli, C., 2010. Long term variations of the Campi Flegrei (Italy) volcanic system as revealed by the monitoring of hydrothermal activity. *J. Geophys. Res.* 115, B03205. <http://dx.doi.org/10.1029/2008JB006258>.
- [9] Chouet, B.A., Julian, B.R. 1985. Dynamic of an expanding fluid filled crack. *J. Geophys. Res.*, 90, 1118711198.
- [10] Chouet B. A. 1996. Long-period volcano seismicity: its source and use in eruption forecasting. *Nature* 380, 309–316, doi:10.1038/380309a0.
- [11] Ciaramella, A., De Lauro, E., Falanga, M., Petrosino, S. 2011. Automatic detection of long-period events at Campi Flegrei Caldera (Italy). *Geophys. Res. Lett.* 38, L18302, doi:10.1029/2011GL049065.
- [12] Cichocki, A., Amari, S., Siwek, K. et al. 2003. ICALAB Toolboxes, <http://www.bsp.brain.riken.jp/ICALAB>.

- [13] Cusano, P., Petrosino, S., Saccorotti, G. 2008. Hydrothermal Origin for Sustained Long-Period (LP) activity at Campi Flegrei Volcanic Complex, Italy. *J. Volcanol. Geoth. Res.* 177, 1035–1044, doi: 10.1016/j.jvolgeores.2008.07.019.
- [14] D’Auria, L., Giudicepietro, F., Aquino, I., Borriello, G., Del Gaudio, C., Lo Bascio, D., Martini, M., Ricciardi, G.P., Ricciolino, P., Ricco, C., 2011. Repeated fluid-transfer episodes as a mechanism for the recent dynamics of Campi Flegrei caldera (1989–2010), *J. Geophys. Res.*, 116, B04313, doi:10.1029/2010JB007837.
- [15] D’Auria, L., Giudicepietro, F., Martini, M., Lanari R., 2012. The 4D imaging of the source of ground deformation at Campi Flegrei caldera (southern Italy), *J. Geophys. Res.*, 117, B08209, doi:10.1029/2012JB009181.
- [16] De Lauro, E., De Martino, S., Falanga, M., Petrosino, S., 2013. Synchronization between tides and sustained oscillations of the hydrothermal system of Campi Flegrei (Italy), *Geochem. Geophys. Geosyst.* 14, 2628-2637.
- [17] De Lauro, E., Falanga, M., Petrosino, S., 2012. Study on the Long-Period source mechanism at Campi Flegrei (Italy) by a multi-parametric analysis. *Phys. Earth Planet. Int.* 206–207, 16–30, 10.1016/j.pepi.2012.06.006.
- [18] De Lauro, E., De Martino, S., Falanga, M., Palo, M. 2009. Decomposition of high-frequency seismic wavefield of the Strombolian-like explo-

- sions at Erebus volcano by Independent Component Analysis. *Geophys. J. Int.* 177, 1399–1406, doi: 10.1111/j.1365-246X.2009.04157.x.
- [19] De Lauro, E., De Martino, S., Falanga, M., Ciaramella, A., Tagliaferri, R. 2005. Complexity of time series associated to dynamical systems inferred from independent component analysis. *Phys. Rev. E* 72, 46712.
- [20] De Natale, G., Troise, C., Pingue, F., Mastrolorenzo, G., Pappalardo, L., Battaglia, M., Boschi, E., 2006. The Campi Flegrei caldera: unrest mechanisms and hazards, 269 (1). Geological Society, London, Special Publications, 25-45. <http://dx.doi.org/10.1144/GSL.SP.2006.269.01.03>.
- [21] De Siena, L., Del Pezzo, E., Bianco, F. 2010. Seismic attenuation imaging of Campi Flegrei: Evidence of gas reservoirs, hydrothermal basins, and feeding systems. *J. Geophys. Res.* 115, B09312, doi:10.1029/2009JB006938.
- [22] Eyre, T.S., Bean, C.J., De Barros, L., Martini, F., Lokmer, I., Mora, M.M., Pacheco, J.F., Soto, G.J., 2015. A brittle failure model for long-period seismic events recorded at Turrialba volcano, Costa Rica, *J. Geophys. Res. Solid Earth*, 2169-9356, doi: 10.1002/2014JB011108.
- [23] Falanga, M., Petrosino, S. 2012. Inferences on the source of long-period seismicity at Campi Flegrei from polarization analysis and reconstruction of the asymptotic dynamics. *Bull. Volcanol.* 74, 1537–1551, doi: 10.1007/s00445-012-0612-2.
- [24] Fraser, A.M., Swinney, H.L. 1986. Independent coordinates for strange attractors from mutual information. *Phys. Rev. A* 33, 1134–1139.

- [25] Hyvärinen, A., Karhunen, J., Oja, E. 2001. Independent Component Analysis, John Wiley & Sons.
- [26] Julian, B.R., 1994. Volcanic tremor: nonlinear excitation by fluid flow. *J. Geophys. Res.* 99, 11859-11877.
- [27] Kao, H., Thompson, P.J., Rogers, G., Dragert, H., Spence, G. 2007. Automatic detection and characterization of seismic tremors in northern Cascadia. *Geophys. Res. Lett.* 34, L16313, doi:10.1029/2007GL030822.
- [28] Kawakatsu, H., Yamamoto, M., 2007. Volcano Seismology. In: Schubert G. (ed.) *Treatise on Geophysics Vol. 4*. Elsevier, Oxford pp 389–420.
- [29] Kennel, M.B., Brown, R., Abarbanel, H.D.I., 1992. Determining embedding dimension for phase space-reconstruction using a geometrical construction. *Phys. Rev. A* 45, 3403–3411.
- [30] Konstantinou, K.I., Schlindwein, V. 2002. Nature, wavefield properties and source mechanism of volcanic tremor: a review. *J. Volcanol. Geotherm. Res.* 119, 161–187.
- [31] Konstantinou, K. I. 2002, Deterministic non-linear source processes of volcanic tremor signals accompanying the 1996 Vatnajökull eruption, central Iceland. *Geophys. J. Int.* 148, 3, 663-675.
- [32] Kumagai, H., Chouet, B.A., 1999. The complex frequencies of long-period seismic events as probes of fluid composition beneath volcanoes. *Geophys. J. Int.* 138, F7F12.

- [33] Kumagai, H., Chouet, B.A., Nakano, M., 2002. Waveform inversion of oscillatory signatures in long-period events beneath volcanoes. *J. Geophys. Res.* 107, 2301, doi:10.1029/2001JB001704
- [34] Küperkoch, L., Meier, T., Lee, J., Friederich, W. 2010. EGELADOS Working Group. Automated determination of P-phase arrival times at regional and local distances using higher order statistics. *Geophys. J. Int.* 181(2), 11591170, doi:10.1111/j.1365-246X.2010.04570.x.
- [35] Matsubara, W., Yomogida, K., 2004. Source process of low frequency earthquakes associated with the 2000 eruption of Mt. Usu. *J. Volcanol. Geoth. Res.* 134, 223240.
- [36] Moni, A., Craig, D., Bean, C.J., 2013. Separation and location of microseism sources. *Geophys. Res. Lett.* 40, 31183122, doi:10.1002/grl.50566.
- [37] Nakano, M., Kumagai, H., Chouet, B.A., 2003. Source mechanism of long-period events at Kusatsu-Shirane Volcano, Japan, inferred from waveform inversion of the effective excitation functions. *J. Volcanol. Geoth. Res.* 122, 149164.
- [38] Neuberg, J., Luckett, R., Baptie, B., Olsen, K., 2000. Models of tremor and low-frequency earthquake swarms on Montserrat. *J. Volcanol. Geoth. Res.* 122, 83104.
- [39] Orsi, G., Civetta, L., Del Gaudio, C., De Vita, S., Di Vito, M., Isaia, R., Petrazzuoli, S.M., Ricciardi, G.P., Ricco, C. 1999. Short term ground deformations and seismicity in the resurgent Campi Flegrei caldera (Italy):

An example of active block-resurgence in a densely populated area. *J. Volcanol. Geoth. Res.* 91, 415–451.

- [40] Pedersen, M.S., Larsen, J., Kjems, U., Parra, L.C., 2008. Convolutional Blind Source Separation Methods, Springer, Handbook of Speech Processing, 1065-1094.
- [41] Petrosino, S., Damiano, N., Cusano, P., Di Vito, M.A., de Vita, S., Del Pezzo, E. 2012. Subsurface structure of the Solfatara volcano (Campi Flegrei caldera, Italy) as deduced from joint seismic-noise array, volcanological and morphostructural analysis. *Geochem. Geophys. Geosyst.* 13, Q07006, doi:10.1029/2011GC004030.
- [42] Rouland D., Legrand D., Zhizhin M., Vergnolle S. 2009, Automatic detection and discrimination of volcanic tremors and tectonic earthquakes: An application to Ambrym volcano, Vanuatu. *J. Volcanol. Geotherm. Res.* 181, 196–206.
- [43] A.C. Rust, K.V. Cashman, P.J. Wallace (2004). Magma degassing buffered by vapor flow through brecciated conduit margins. *Geology*, 32, 349352, <http://dx.doi.org/10.1130/G20388.2>
- [44] Saccorotti G., Petrosino S., Bianco F., Castellano M., Galluzzo D., La Rocca M., Del Pezzo E., Zaccarelli L., Cusano P. 2007. Seismicity associated with the 2004-2006 renewed ground uplift at Campi Flegrei Caldera, Italy. *Phys. Earth Planet. Int.* 165, 14–24.
- [45] Saccorotti, G., Bianco, F., Castellano, M., Del Pezzo, E., 2001. The

JulyAugust 2000 seismic swarms at Campi Flegrei volcanic complex, Italy. *Geophys. Res. Lett.* 28, 25252528.

- [46] Thun, J., Lokmer, I., Bean, C.J., 2015. New observations of displacement steps associated with volcano seismic long-period events, constrained by step-table experiments. *Geophys. Res. Lett.* 42, 38553862.

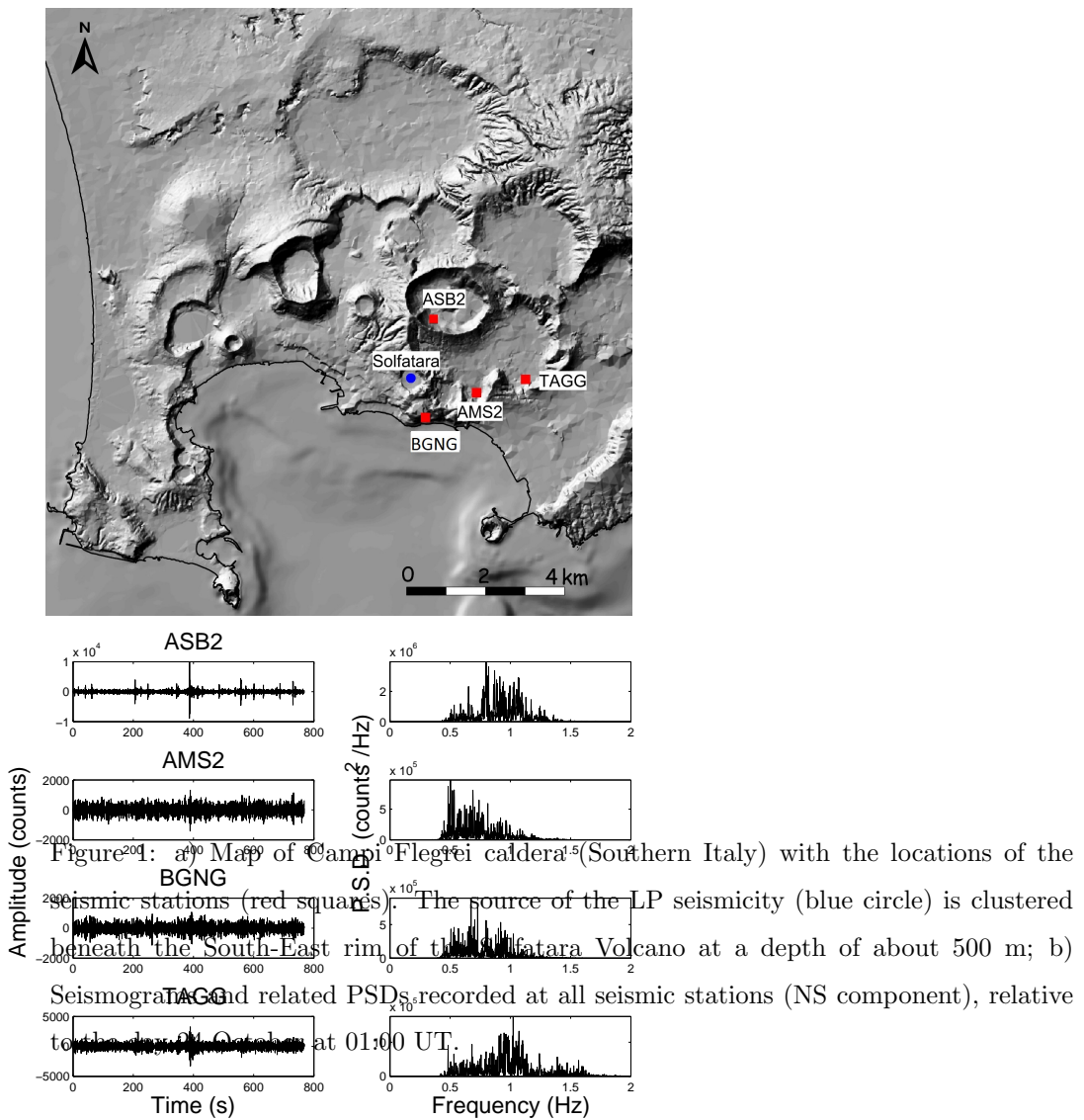


Figure 1: a) Map of Campi Flegrei caldera (Southern Italy) with the locations of the seismic stations (red squares). The source of the LP seismicity (blue circle) is clustered beneath the South-East rim of the Solfatara Volcano at a depth of about 500 m; b) Seismogram and related PSDs recorded at all seismic stations (NS component), relative to the onset of the event at 01:00 UT.

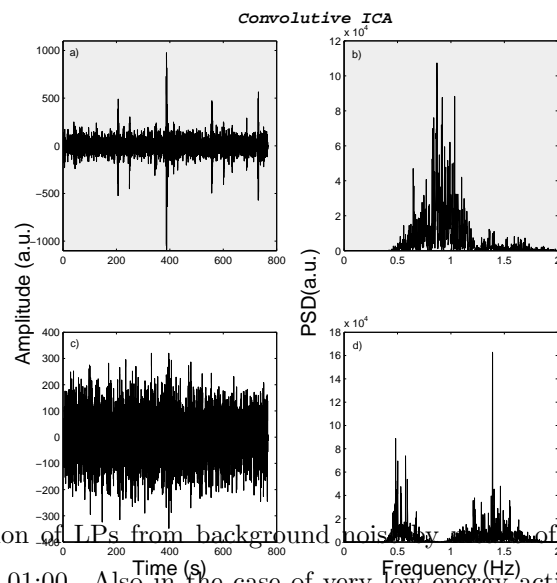


Figure 2: Separation of LPs from background noise by means of CICA relative to the day 24 October at 01:00. Also in the case of very low energy activity and hence of low signal-to-noise ratio (SNR), the CICA approach permits to obtain a better result. Indeed, from PSDs we can discriminate two fundamental frequency bands, one associated with the LP seismic signals, typically peaked around 0.8 Hz, and another with a broader spectral content associated to the ambient noise (contribution of both the meteo-marine component (peak below 1 Hz) and the anthropogenic activity (peak at 1.5 Hz)).

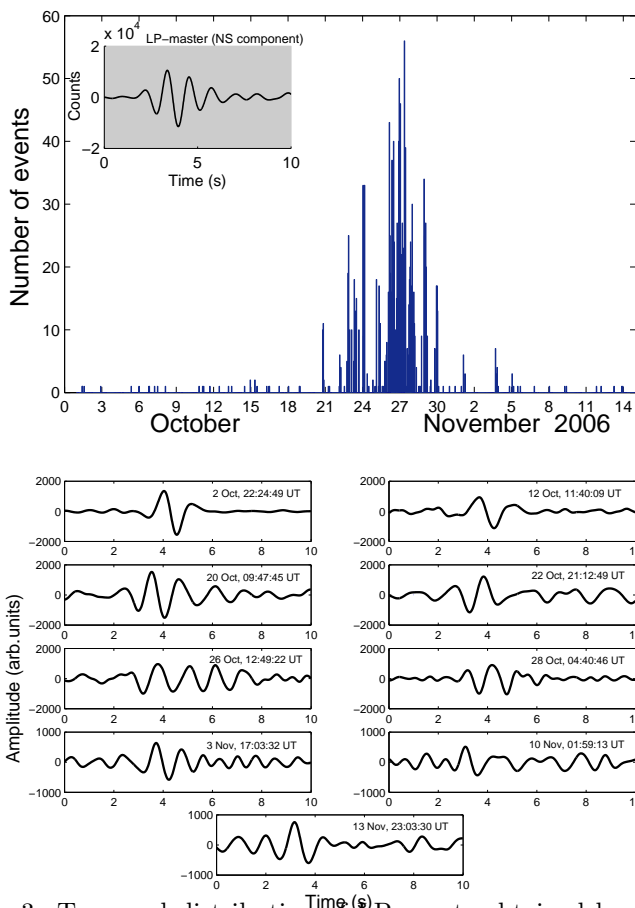


Figure 3: Temporal distribution of LP events obtained by the automatic picking of the CICA time series considering the entire period; each bar of the histogram corresponds to 1-h-long interval. About 1700 LPs with high correlation coefficients with respect to an LP master event are extracted spanning a period from the beginning to October until mid November. The inset shows the LP master event recorded at the Station ASB2, North-South component (it occurred on 26 October at 12:18:15 UT). The lower panel shows a subset of nine LP waveforms taken all along the period representative of the seismic crisis.

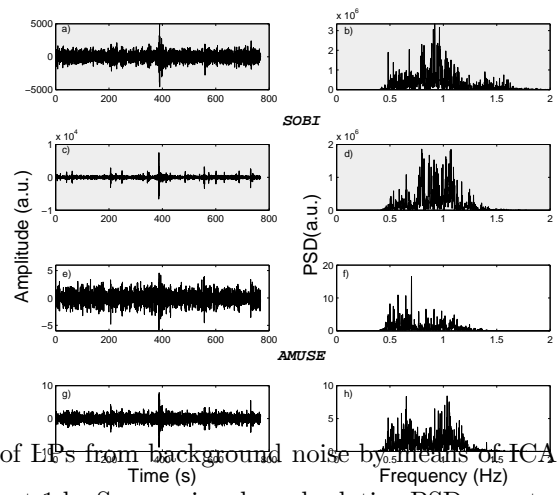


Figure 4: Separation of EPs from background noise by means of ICA algorithms relative to the day 24 October at 1 h: Source signals and relative PSD as extracted by SOBI (a-d) and AMUSE (e-h).

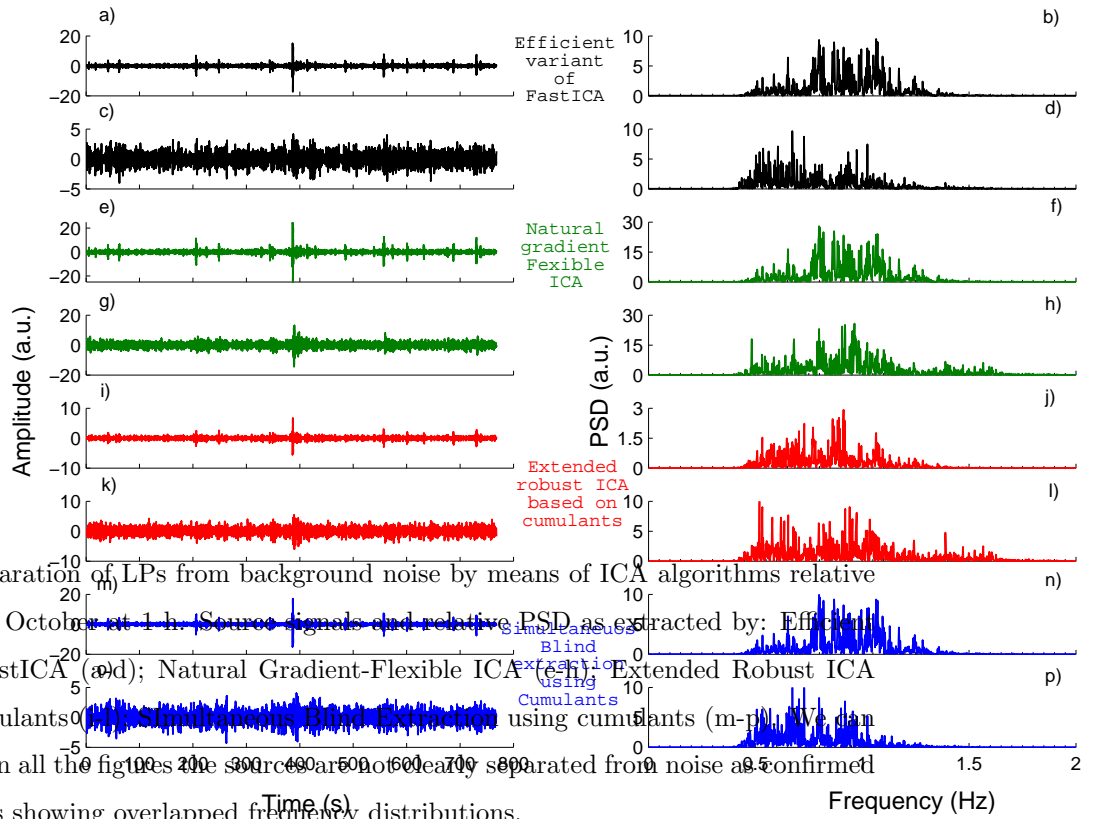


Figure 5: Separation of LPs from background noise by means of ICA algorithms relative to the day 24 October at 1 h. Source signals and relative PSD as extracted by: Efficient Variant of FastICA (a-d); Natural Gradient-Flexible ICA (e-h); Extended Robust ICA based on cumulants (i-l); Simultaneous Blind Extraction using cumulants (m-p). We can observe that in all the figures the sources are not clearly separated from noise as confirmed by their PSDs showing overlapped frequency distributions.

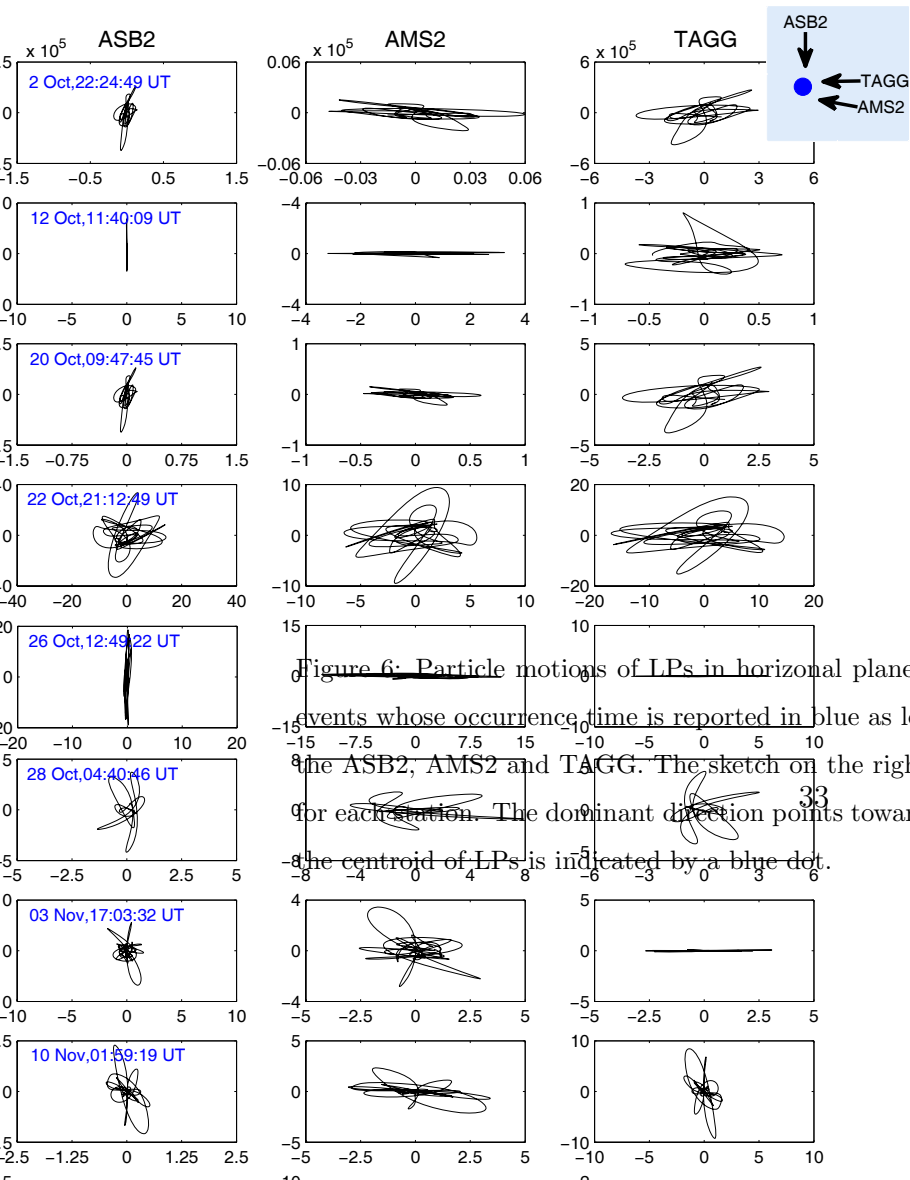


Figure 6: Particle motions of LPs in horizontal planes. The rows are relative to selected events whose occurrence time is reported in blue as legend, whereas the columns indicate the ASB2, AMS2 and TAGG. The sketch on the right shows the directions of the source for each station. The dominant direction points towards the Solfatara (see the inset where the centroid of LPs is indicated by a blue dot).

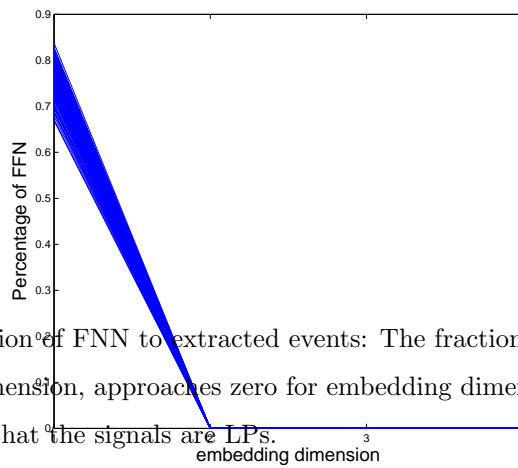


Figure 7: Application of FNN to extracted events: The fraction of FNN, as a function of the embedding dimension, approaches zero for embedding dimension equal to two: this is a clear indication that the signals are LPs.